Heat and mass transfer to active particles in fluidized beds — An update

Citation for the original published paper (version of record):
Leckner, B. (2027). Heat and mass transfer to active particles in fluidized beds — An update. Powder Technology, 485. http://dx.doi.org/10.1016/j.powtec.2026.122995

(article starts on next page)

Powder Technology 485 (2027) 122995

Contents lists available at ScienceDirect

Powder Technology

journal homepage: www.journals.elsevier.com/powder-technology

Heat and mass transfer to active particles in fluidized beds — An update

Bo Leckner

Division of Energy Technology, Chalmers University of Technology, 41296 Göteborg, Sweden

HIGHLIGHTS

- The article deals with transport processes in a fluidized bed.
- Heat and mass transfer between bed particles and active particles is investigared.
- Expressions using Archimedes number are converted to Reynolds number.
- The dependence of *Nu* on velocity is described approximately.

GRAPHICAL ABSTRACT

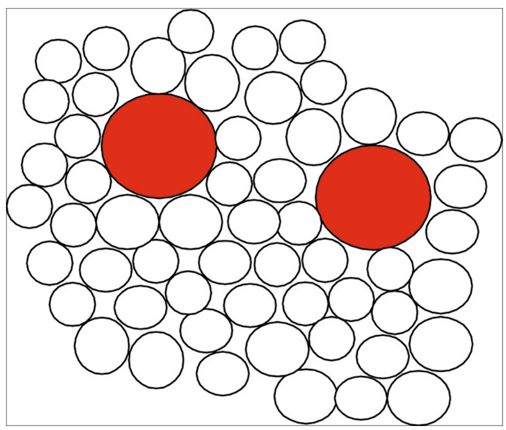

ARTICLE INFO

Keywords:
Fluidized bed
Particle heat transfer
Particle mass transfer
Active bed particles

ABSTRACT

In previous investigations, heat and mass transfer to or from active particles in a fluidized bed of inert particles are described based on correlations involving the Archimedes number (*Ar*). Since many users are accustomed to relationships from single-phase flow where Reynolds number (*Re*) is the parameter involved in heat and mass transfer correlations, it could be of interest to translate the expressions from *Ar* to *Re*. This is the purpose of the present work, which uses well-known relationships for minimum and optimum fluidization velocities to convert *Ar* into *Re*. As a result of this transformation, the influence of gas velocity becomes obvious, and that is also elucidated by describing the heat transfer at velocities above and below the optimum velocity.

1. Introduction

Archimedes number (*Ar*) is often used in heat and mass transfer correlations for fluidized bed. In a fluidized bed, consisting of Group A or B particles, the fluid dynamics are affected by the relation between the drag force from the gas on a particle or on a group of particles and the gravity acting on these particles. When the gas velocity takes the value of the minimum fluidization velocity and the bed is just fluidized, there is a balance between the drag and the gravity forces. *Ar* expresses such balanced situations, strongly dependent on particle size, while Reynolds number (*Re*) contains both fluidization velocity and particle size. Other phenomena, such as the optimum velocity, i.e. the gas velocity at maximum heat transfer, the velocity at the onset of turbulent fluidization, and the transport velocity, are usually also related to *Ar*.

Fig. 1 presents the connection between minimum fluidization

E-mail address: ble@chalmers.se.

https://doi.org/10.1016/j.powtec.2026.122995
Received 15 February 2026; Received in revised form 20 May 2026; Accepted 19 July 2026
Available online 7 August 2026

Nomenclature

Latin symbols

a	Thermal diffusivity, $k/(\rho c_p)$, m^2/s
d	Particle dimension, m, mm, or μm
C_1, C_2	Coefficients
c_p	Specific heat, J/(kg·K)
D_h	Hydraulic diameter, m
D	Mass diffusivity, m^2/s
F	Force, N/m^2
$f()$	Function
h	HTC heat-transfer coefficient, W/m^2K
g	Acceleration of gravity, m/s^2
k	Thermal conductivity, W/mK
Q	Heat flow, W
W	Radius of particle, m
T	Temperature, K
u	Fluidization, superficial velocity, m/s
v	Local velocity $v = u/\varepsilon$, m/s

Greek symbols

β	Mass transfer coefficient, m/s
ΔH	Height, height difference, m
ΔP	Pressure drop, N/m^2 or Pa
ε	Voidage, *mf* minimum fluidization, *e* emulsion, particle phase, –
φ	Sphericity, –
ν	Kinematic viscosity, m^2/s
μ	Dynamic viscosity, Ns/m^2, kg/(m,s)
ξ	Resistance coefficient, –
ρ	density, gas *g*, particle *p*, kg/m^3

Indices

a	active particle
eff	effective quantity
g	gas
gc	gas convection
h	hydraulic
i	inactive, bed particle
max	maximum heat transfer
max,a	maximum heat transfer for an active particle of dimension d_a
mf	minimum fluidization velocity
opt	optimum velocity
pb	packed bed
pc	particle convection
0	conduction, diffusion
1	either *i* or *a* when $d_i = d_a$
+	external, fictitious, spherical surface
∞	maximum conditions

Dimensionless quantities[1]

Archimedes number $Ar = d_i^3(\rho_i - \rho_g)\rho_g g/\mu^2$

Nusselt number $Nu_x = d_x h/k_g$, x = i (inert) or a (active); x = ∞ maximum heat transfer

Prandtl number $Pr = \nu\rho_g c_{pg}/k_g$

Reynolds number $Re_x = u_x d\rho_g/\mu$; $x = mf$ ---minimum fluidization velocity u_{mf}, $x = opt$---optimum velocity corresponding to maximum heat transfer, $x = i$ at $d = d_i$; $x = a$ at $x = d_a$

Schmidt number $Sc = \nu/D$

Sherwood number $Sh_x = d_x\beta/D$, β diffusion coefficient, D gas diffusivity, x same as for Nu

Superscripts

n, m	various cases

Abbreviations

B&P	Baskakov-Palchonok (model)
CFB	Circulating fluidized bed

[1] The index on *Re, Nu*, *Sh*, *Ar* should be *i*, if related to the inert bed particle. This is generally the case, and indices are only inserted if it is not *i* or to mark other situations.

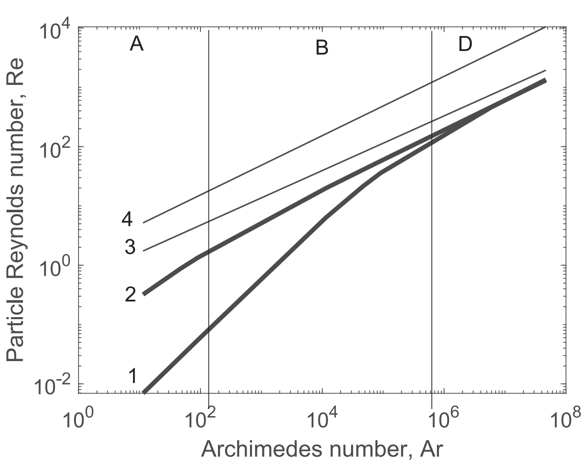

Fig. 1. Connections between *Re* and *Ar*. 1) Minimum fluidization velocity Re_{mf}, Eq. 4; 2) Optimum velocity Re_{opt}, Eq. 7; 3) Transition from bubbling to turbulent $Re_c = 0.565\ Ar^{0.461}$ (absolute pressure measurements) [1]; 4) Initiation of significant entrainment $Re_{se} = 1.53\ Ar^{0.5}$ [1]. A, B, and D are regions of Geldard's classes whose limits are determined by Grace [1] for sand-like particles in air-like gas.

velocity (Re_{mf}), optimum velocity (Re_{opt}), and *Ar*. For comparison, also the velocity denoting the transition to turbulent fluidization and the "velocity of significant entrainment" are included in the figure. Especially for beds of Group B particles there are many proposals of correlations for the transition to turbulent fluidization [2]. Among others, the vessel diameter is mentioned as an influencing factor. In commercial large-size fluidized beds. Operating with Group B particles, the turbulent regime may never be attained. The beds stay bubbling even at high velocity if there is sufficient bed material to form a bottom bed in a circulating system [3].

Geldart's particle-size classes are indicated in the diagram. Group B particles according to Geldard's classification are important because they are common in applications of solid-fuel conversion. Group B particles extend from about $Ar = 125$ to 145,000, yielding $Re_{mf} = 0.08$ to 50 as derived by Eq. (4). The range of $Re_{i,opt} = 1.6$ to 72 is given by Eq. (7). For small *Re*, i.e. particles of Group A, conduction is more important than gas convection.

The relationships between *Ar* and *Re* explain why *Ar* is often used in fluidized-bed heat and mass transfer correlations. This was particularly common in the former Soviet Union. However, the single-phase representations are common in the minds of many users; *Re* times *Pr* or *Sc* often expresses the heat or mass convection. Therefore, the present work investigates the possibility of substituting *Ar* with *Re* in heat and mass transfer relationships related to active particles in a fluidized bed of passive (inert) particles. The treatment follows a review on this topic [4], relying on the findings from the Soviet researchers Baskakov and Palchonok, working independent of each other, but inspired by the same scientific environment. The method indicated or proposed by these scientists for the estimation of heat and mass transfer coefficients has been summarized in [4] where details and further information can be found, including comparisons with other work on heat and mass transfer to active particles in a fluidized bed. It treats active and inert particles of dimensions d_a and d_i, respectively, by interpolation between empirical correlations, derived for the limiting cases of $d_a = d_i$ and $d_a >> d_i$. The present work focusses on the transformation of the available heat and mass transfer correlations from *Ar* to *Re*. and on the dependency on velocity. Here, the works of Baskakov and Palchonok are treated together, called the B&P model.

2. Transformation from *Ar* to *Re*

2.1. Heat and mass transfer at the interpolation limit $d_a = d_i$

The heat transfer to an active spherical particle in a bed of inert particles of the same size is caused by conductive and gas convective mechanisms. It can be written [4,6].

$$Nu_1 = Nu_0 + 0.117 Ar_i^{0.39} Pr^{0.33} \tag{1}$$

The first term on the right-hand side, Nu_0, is the heat conduction to a particle in a particle phase with a voidage ε and a solids concentration of 1-ε, derived in the same way as for single-phase flow, but accounting for the contribution of the surrounding inert particles. A description and a discussion are presented in App A.

The conductive term, Eq. (A6), gives a value of Nu_0 of about 10 for a voidage at minimum fluidization velocity ε_{mf} around 0.4–0.5, to be compared with Nu_0 of 6 as obtained through a different derivation by Palchonok et al. [6] for a dense packing of particles. The advantage of Eq. (A6) is that it goes towards the single-phase value of 2 if the voidage approaches unity, if $\varepsilon = \varepsilon_{mf}$ is relaxed and $\varepsilon \rightarrow 1$ like in the transport zone of a circulating fluidized bed combustor. However, the description of the voidage around the active particle is uncertain, and comparison with measurement data on heat transfer [4,6] indicates that a value of 6 fits better than 10 for application of solid fuel conversion in dense fluidized beds.

The second term of Eq. (1) is the contribution of heat transfer by gas convection to an active particle of the same size as the inert bed particles, obtained by fitting to available data [6], assuming that in the $d_a = d_i$ case there is gas convection but no particle convection (because the relative movement of particles is small). An expression for mass transfer to an active particle in a bed of inert particles was derived by comparison with experimental data [6],

$$Sh_1 = 2\varepsilon_{mf} + 0.117 Ar_i^{0.39} Sc^{0.33} \tag{2}$$

The two terms of this equation represent mass transfer by gas diffusion and gas convection. The similarity of the mass-convection term and the corresponding heat-transfer term in Eq. (1), supported by measured data, presumes that at $d_i = d_a$ the contribution of particle convection to heat transfer is negligible, so both correlations Eqs. (1,2) are affected by the gas in a similar way, making the contributions of gas convection equal according to the analogy of heat and mass transfer. However, the conduction terms differ. In the mass transfer case, the surrounding particles impede the transfer by occluding the active particle. Avedesian and Davidson [7] proposed a correction by means of the voidage of the surrounding particle suspension ε_{mf}. This is used in Eq. (2).

In this case of equal particle sizes (and reasonably similar particle densities) the active particle is contained in an environment of inert particles, forming the particle phase of the fluidized bed. The heat and mass transfer takes place as if in an incipiently bubbling fluidized bed at u_{mf}, while the fluidization velocity in the bed could be above u_{mf}. The active particles are part of the particle phase (only at high velocities some particles may pass the bubble phase). The classical two-phase theory of fluidization states that the excess gas above what is needed for fluidization, forms bubbles, and the particle phase remains in minimum fluidization conditions. However, many investigations have shown that more gas passes the bed than what corresponds to (visible) bubbles and the emulsion phase. The conclusion is that a certain gas-flow passes the bed in the form of a through-flow, either through the bubbles or through the particle phase. It has been difficult to determine the repartition of the through-flow between the two phases, and various results have been presented for the particle phase. Generally, with Group A particles, the particle phase expands above ε_{mf} at higher fluidization velocities, indicating a through-flow through the particle phase. For instance, Abrahamson and Geldart [8] have proposed a correlation to describe the gas velocity in this case. It is more uncertain to reach a firm conclusion for Group B particles. *Bi* and Su [9] found that the flow through the particle phase was equal to u_{mf} until a high fluidization velocity was attained, when the fluidization changed from bubbling to turbulent in the narrow laboratory reactor used. The state of minimum fluidization in the particle phase in beds of Group B particles has also been claimed or assumed by Geldart [10] and Baeyens and Wu [11]. On the other hand, some investigations found an increase of the through-flow through the particle phase at increasing fluidization velocities and decreasing bed particle size [12–14]. Furthermore, it was observed that the voidage, and then the through-flow of gas through the bed, was considerably higher than ε_{mf} in the vicinity of the porous or perforated distributors used (within a range of one to two decimetres above the bottom). At higher levels in the bed, the voidage approached that of minimum fluidization [12,13,15]. This could explain why Yates et al. [16] observed minimum fluidization in the particle phase outside of the more disperse layer surrounding the bubble studied: this bubble was selected at 0.3 m or higher above the distributor plate. Finally, Werther and Wein [17] investigated various properties of high-velocity beds, among others the voidage of the dense phase, see Fig. 2, where there is an initial jump in voidage from a small velocity above minimum fluidization of $\varepsilon = 0.45$ to about $\varepsilon = 0.5$ that is typical for the state of fluidization in the investigations defining the $d_a = d_i$ case. The diagram shows that the further development of the voidage in the particle phase with velocity is quite small despite the high velocities involved. Even though the bed voidage increases as the bed expands at higher velocities, the voidage of the particle phase remains relatively constant. (The title of [17] claims that it deals with a turbulent bed. However, this was just assumed by the authors without any verification. In fact, they conclude that they found "no changes in the fluidization characteristics when the

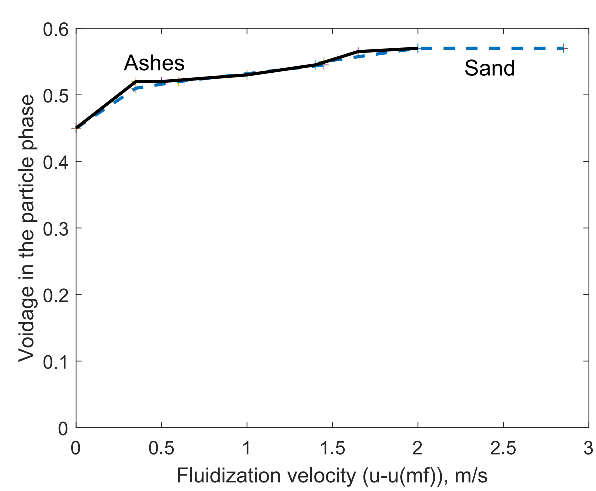

Fig. 2. The voidage of the particle phase in bubbling beds of sand or ashes as a function of the fluidization velocity above u_{mf}, Werther and Wein [17].

gas velocity increased from bubbling to turbulent". So, obviously, the bed was not turbulent).

There are more results pointing at the conditions in the particle phase. Collier et al. [18] measured the heat transfer to a particle of the same size as the bed particles during an increase in velocity from a packed bed to a bubbling bed and found that the heat transfer increased up to u_{mf} and then remained quite constant at higher velocity, indicating a heat transfer like that at u_{mf}. A computational study by Zhou et al. [19] shows the same results.

The impact of conductive and convective heat transfer is shown by the ratio of the two terms in Eq. (1). This ratio becomes,

$$\text{Ratio} = Nu_0 / \left(Ar^{0.39}\, Pr^{0.33}\right) \tag{3}$$

Ar is translated into *Re* (the inert particle size) for the conditions of the particle phase, as shown in §2.2. The ratio of Eq. (3) is large at small *Re* (the gas convection term is insignificant), while it decreases with increasing *Re* to become around unity at *Re* ➔ 1. The ratio continues to fall with further increase in *Re*, meaning that the importance of the convection term increases. For *Sh* (Eq. 2) the ratio is lower than in the case of *Nu* and the conduction term is less important than the convection term compared with the heat transfer case. This difference between *Nu* and *Sh* contrasts from single-phase cases where heat and mass transfer are similar. As obvious from the heat transfer case, the ratio in Eq. (3), decreases with an increase in the voidage, whereas for mass transfer there is a slightly opposite trend.

In summary: while moving around in the particle phase of a fluidized bed, an active particle of a similar size as the bed particles experiences a condition like that of minimum fluidization. Therefore, the assumption that it is exposed to a gas flow of u_{mf} can be considered reasonable for the $d_i = d_a$ case: 1) for Group A particles the conduction component is the most important one, and differences affecting the convective component are less significant; 2) for Group B particles, there is certainly a special situation close to a porous or perforated gas distributor, but the particle moves around in the bed and is most of the time in regions whose emulsion phase is close to the u_{mf} state, even if the overall fluidization velocity u is higher than u_{mf}.

2.2. Transformation from Ar to Re at $d_a = d_i$

As derived in App B, the Ergun equation [20] with data from Wen and Yu [21] provides a relationship between *Ar* and *Re* under minimum fluidization conditions,

$$Ar = 1650Re_{mf} + 24.5{Re_{mf}}^2 \text{ or } \mathrm{Re}_{mf} = -33.7 + \sqrt{33.7^2 + 0.0408Ar} \tag{4}$$

Ar inserted in Eqs. (1) and (2) gives,

$$Nu_1 = \mathrm{Nu}_0 + \left[6.73\mathrm{Re}_{mf} + 0.10\mathrm{Re}_{mf}^2\right]^{0.39} Pr^{0.33} \tag{1a}$$

$$Sh_1 = 2\varepsilon_{mf} + \left[6.73\mathrm{Re}_{mf} + 0.10\mathrm{Re}_{mf}^2\right]^{0.39} Sc^{0.33} \tag{2a}$$

2.3. Analysis of the case $d_a = d_i$

It was claimed that, because the active particle is contained in the particle phase of the bubbling bed, Eq. (1) represents heat transfer under minimum fluidization conditions. Then, it is about independent of the overall fluidization velocity and can be compared with the gas convective heat transfer described by the correlations of Baskakov and Suprun [22] and of Baskakov et al. [23]. These data also represent gas convection, since they were transformed from measurements of mass transfer to a cylinder in a fluidized bed, mentioned in App C. Furthermore, Čatipović [24] made a set of high-quality measurements, valid for heat transfer to a horizontal tube in a bed under just-fluidized conditions, covering a wide range of bed particle-sizes. Čatipović data agree with those of Baskakov and coworkers. Correlations representing the transition from a packed to a fluidized bed, for instance, that of Wakao et al. [25] for $u = u_{mf}$, express heat transfer to bed particles in a just-fluidized bed and agree with Palchonok's gas-convection data related to particles of the same size. There is a difference between the two data sets as shown by Fig. 3. One set represents the gas-convective heat transfer to a particle in a bed with particles of the same size, whereas the other sets concern gas convection heat-transfer to larger objects in the bed. To focus on gas convection, Fig. 3 only shows the convective terms. There is a considerable difference between the two curves in Fig. 3; the upper curve describes a more efficient heat transfer than the lower one, which is recorded for heat transfer on larger bodies where the driving temperature or concentration difference grows smaller during the contact than in the case of $d_a = d_i$.

2.4. The interpolation limit for large active particles, $d_a >> d_i$

The maximum heat transfer is a result of the movement of bed particles at the surface of the active particle. The simultaneous gas convection is added and is otherwise not related to the particle convection, the latter being the dominant mechanism of heat transfer for a wide range of smaller bed particles, Fig. 4.

The maximum heat transfer to a large, rounded object with dimension d_a in a fluidized bed of inert particles d_i depends on both particle and gas convection. Baskakov et al. [23] proposed,

$$Nu_\infty = Nu_{pc} + Nu_{gc}$$

that is, with *Nu* and *Sh* related to d_i,

$$Nu_\infty = 0.86Ar^{0.20} + 0.009Ar^{0.5}\, Pr^{0.33} \tag{5}$$

In mass transfer, only gas convection takes place, Baskakov and Suprun [22],

$$Sh_\infty = 0.006Ar^{0.5}\, Sc^{0.33} \tag{6}$$

The gas convection terms in Eqs. (5, 6) are the same, obeying the analogy between heat and mass transfer, so the mass transfer data were also used for the heat transfer correlation. Details in the conversion from correlations of mass to heat transfer and the interpretation of the gas convection component are discussed in App C. The particle convection correlation represents data under the optimum condition [23], whereas the gas convection has been derived at velocities above the optimum

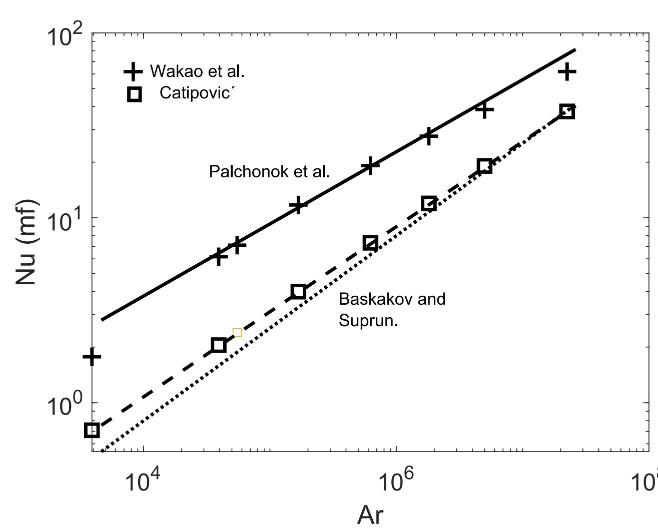

Fig. 3. The gas convection part of Palchonok's correlation for $d_a = d_i$ Eq. (1) and other correlations for gas convection on a bed-particle level (Wakao et al. [25], +) compared to gas convective heat transfer to larger objects in the bed, measured by Baskakov & Suprun [22] (.......) and Čatipović [24] (□).

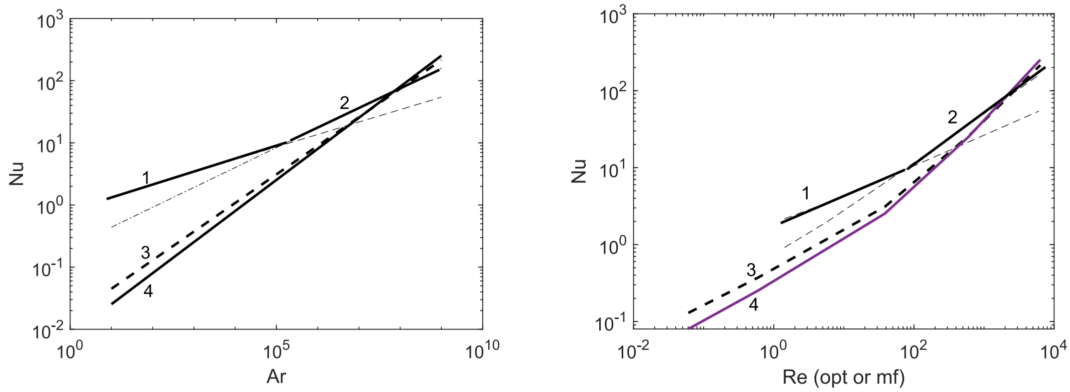

a) b)

Fig. 4. a) Nusselt number, Nu_{max} for maximum heat transfer vs. Ar. b) The same, related to *Re;* 1 and 2 to Re_{opt} and 3 and 4 to $Re_{mf,}$ converted from *Ar* by Eqs. (4, 7). The range of *Ar* and, hence also of *Re,* is extended beyond normal application to illustrate the relationships. Extrapolations of the relationships 1 and 2 are shown as dashed-dotted lines.

1. $Nu_{pc} = 0.86Ar^{\ 0.20}$. Particle convective, Varygin and Martyushin quoted by [23], Eq. (5).
2. $Nu_{pc} = 0.21Ar^{\ 0.32}$. Particle convective, at high *Ar*, [23].
3. $Nu_{gc} = 0.0175Ar^{\ 0.46}Pr^{0.33}$. Gas convective, [22], App C.
4. $Nu_{gc} = 0.009Ar^{\ 0.5}Pr^{0.33}$. Gas convective, improved fit, [23] Eq. (5), App C.

condition [22]. Because the active particle is present in the particle phase, the gas convection is determined by the minimum fluidization of the particle size concerned, so *Ar* in Eq. (5) is transformed into both Re_{opt} and Re_{mf}. This will be further discussed below. The gas conduction terms in Eqs. (5, 6) are neglected because the term d_i/d_a converting the correlations from base d_a to d_i is very small when d_a is large.

Re for maximum (optimum) particle convection, expressed with the superficial velocity u_{opt}, was determined by Aerov and Todes [26], mentioned by Gelperin and Ainshtain [27],

$$Re_{opt} = Ar \Big/ \left(18.0 + 5.22Ar^{0.5}\right) \text{ or } Ar = \left[2.61\mathrm{Re}_{opt} + \sqrt{\left(2.61\mathrm{Re}_{opt}\right)^2 + 18\mathrm{Re}_{opt}}\right]^2 \quad (7)$$

With *Ar* from Eq. (7) inserted into Eqs. (5, 6), the expressions are converted into Re_{opt}, valid for particle convection. The gas convection term in Eq. (5) is transformed by *Ar* from Eq. (4), valid at minimum fluidization.

$$Nu_\infty = 0.86\left[2.61\mathrm{Re}_{opt} + \sqrt{\left(2.61\mathrm{Re}_{opt}\right)^2 + 18\mathrm{Re}_{opt}}\right]^{0.40} + 0.009\left(1650\mathrm{Re}_{mf} + 24.5\mathrm{Re}_{mf}^2\right)^{0.5} Pr^{0.33} \quad (5a)$$

$$Sh_\infty = 0.006\left(1650\mathrm{Re}_{mf} + 24.5\mathrm{Re}_{mf}^2\right)^{0.5} Sc^{0.33} \quad (6a)$$

Fig. 4 shows the various expressions for heat transfer in the large active-particle case.

2.5. Simplifications

The replacement of the convective terms in Eqs. (1a, 2a) with a simple power law of the form $\mathrm{const}_1\mathrm{Re}^{\mathrm{const2}}$, yields.

$$Nu_1 = \mathrm{Nu}_0 + 2.12Re_{mf}^{\ 0.45}\ Pr^{0.33} \quad (1b)$$

$$Sh_1 = 2\varepsilon_{mf} + 2.12\mathrm{Re}_{mf}^{0.45}Sc^{0.33} \quad (2b)$$

Index 1 could be *a* or *i*, because $d_a = d_i$ in this case. The difference between the exact and the approximate forms is small at high *Re* but greater, although less important, at low *Re*. In the establishment of the correlations for $d_i = d_a$ [6] a relationship of Goroshko et al. [quoted by 40] was used (The same as Aerov and Todes [26]). Goroshko et al. simplified Ergun's expression and introduced $\varphi = 1$ and $\varepsilon = 0.4$ to obtain.

$$\mathrm{Re}_{mf} = \frac{Ar}{1400 + 5.22Ar^{0.5}} \text{ or } Ar = \left[2.61\mathrm{Re}_{mf} + \sqrt{\left(2.61\mathrm{Re}_{mf}\right)^2 + 1400\mathrm{Re}_{mf}}\right]^2 \quad (4a)$$

The deviation of the results from Eq. (4), caused by this correlation, is minor in the range of *Ar* of primary interest. Eq. (7) simplifies to Eq. (7a), whose accuracy is seen in Fig. 8.

$$Re_{opt} = 0.12Ar^{0.55} \text{ or } Ar = 47\mathrm{Re}_{opt}^{1.82} \quad (7a)$$

Eqs. (7a, 4) inserted in Eqs. (5, 6) give.

$$Nu_\infty = 1.86\ Re_{opt}^{\ 0.36} + \left(156.5\ Re_{mf} + 2.3\ Re_{mf}^{\ 2}\right)^{0.5}\ Pr^{0.33} \quad (5b)$$

$$Sh_\infty = \left(127.8\ Re_{mf} + 1.9\ Re_{mf}^{\ 2}\right)^{0.5} Sc^{0.33} \quad (6b)$$

For small *Re*, the $Re_{mf}^{\ 2}$ term can be neglected.

There is no mechanism for particle contribution to mass transfer, and Eq. (6b) is valid over the entire range of *Re*. Despite its small value, it could be reasonable to add the conduction (diffusion) term 2ε, derived for an active particle (App A), related to Sh_i, and therefore corrected by d_i/d_a, inserted to facilitate plotting over a wide parameter range,

$$Sh_\infty = 2\varepsilon\ d_i \Big/ d_a + \left(127.8\ Re_{mf} + 1.9\ Re_{mf}^{\ 2}\right)^{0.5}\ Sc^{0.33} \quad (6c)$$

3. Comments

3.1. Ranges of validity

The expression of the maximum (particle convective, first part of Eq. 5) heat transfer is valid for $30 < Ar < 2{*}10^5$ [23], and can be extended in a modified form up to high *Ar*, as seen from Line 2 in Fig. 4. The translation function $Re_{opt} = f(Ar)$ can be inserted in Eqs. (5, 6) directly in the form of Eq. (7) or in the simplified way, Eq. (7a). There are several similar correlations for the particle convection at maximum heat transfer (Zabrodski [28], Shah [29], Saxena [30]). The choosen correlation, Eq. (7), is deemed to be the best available.

3.2. The form of the correlations

The simple Ar^n expression has been replaced by a more complex form in *Re*, involving several terms. With some approximation, the expression in *Re* could also be represented by a simple power law, a single term, such as Re^m, as shown in Eq. (1b), and for the large particle limit, Eq. (7a). The reason to prefer the more complex second-degree expression in *Re*, such as Eqs. (1a, 2a), is that it is based on a well-known relationship, the Ergun equation, joined with a similarly well-known formulation in terms of the Wen and Yu correlation [21]. The advantage is found in the coefficients C_1 and C_2 (App B) that include important parameters, such as spherisity φ, describing the shape of the particles, and voidage ε_{mf} that also depends on particle conditions like size and size distribution. This opens up for the possibility of chosing other coefficients than those of [21], should that be motivated by the case studied.

3.3. On the validity of the conduction term for heat transfer

The conduction term for heat transfer in Eq. (A6) is about 10 for emulsion phase voidages of about 0.5. This seems high in comparison with measurement data [4,6] where a value of 6 appears most adequate. Eq. (A6) could give a value of about 6 if the voidage were about 0.7, which could be the case locally, close to a surface [31], but the evaluation of its general significance requires computerized investigation. In any case, a value of 6 is recommended for particles of the same size in normaly bubbling beds, and other values could occur only in special situations. The value of 6 was supported by extrapolation of heat transfer data from rather large *Re* to zero [4]. Collier et al. [18] extrapolated from a large *Re* to $Re = 0$ and obtained a value of $Nu = 2$ at $Re = 0$. However, there is an uncertainty in extrapolation. The data of Collier et al. can also be extrapolated to a conduction of 6. The data are clearly shown, and the evaluation can be assessed by a reader.

The exact magnitude of the conductive term for heat transfer may be uncertain, but qualitatively it can be concluded that the particles surrounding an active particle have a higher thermal conductivity than the gas, and this enhances the conductive heat transfer. Therefore, *Nu* related to d_a is always larger than the single-phase value of 2 as long as there are particles present in the surrounding of the active particle. This is just opposite to mass transfer, where the surrounding particles reduce the mass transfer to below 2. The conduction term is most significant during heat exchange of a particle of the same size as the bed particles. As shown in App A (Eq. A8) it may be insignificant for a large particle in a bed of smaller particles if *Nu* and *Sh* are related to d_i.

4. Influence of velocity

The transition to *Re* makes the influence of velocity evident. In single-phase flow, heat and mass transfer are exposed to velocity in the same way, in the form of gas convection. In the fluidized bed, there is also a contribution to heat transfer by the particles, whereas the mass transfer is only affected by the gas convecion.

4.1. Gas convection

Gas convection influences both heat and mass transfer. The analogy of heat and mass transfer is the basis for the establishment of Eqs. (1, 2) that have the same form, although the data used originate from different sources. Likewise, the analogy was utilized by Baskakov and Suprun [22], App C, yielding the same expression for heat and mass transfer. Above, and in App C, it is stated that the convection between gas and active particles takes place predominantly in the particle phase. Fig. 2 shows that the density of this phase remains rather independent of the fluidization velocity, only subjected to u_{mf}. The data of [22] (Fig. C1) also support this observation. Hence, the gas convection components of both heat and mass transfer are only influenced by Re_{mf}, related to the inert particle size through *Ar*, as expressed by Eq. (4).

Often mass transfer relationships are presented in a form that reminds of a single-phase correlation (Agarwal and La Nauze [32], Table 4), leading to an expression,

$$Sh = 2\varepsilon + 0.69Re^{0.5}\ Sc^{0.33} \tag{8}$$

The local gas velocity in the bed, inserted into *Re*, is $v = u/\varepsilon$, based on the fluidization velocity *u*. In this form, it was found difficult to predict measured data, and various approaches, involving the bubble characteritics, were tried [32]. Later, Scala [33] sucessfully validated the same relationship, using $v = u_{mf}/\varepsilon_{mf}$ in *Re* and $\varepsilon = \varepsilon_{mf}$ in the conductive term. This proved that the active particles predominantly remain in the particle phase subjected to u_{mf}. Occational excursions of thr active particle into the bubble phase do not significantly impact on the total mass transfer, even though the velocity were between the minimum and optimum velocities (where the particle convective heat transfer is affected by the gas velocity). Also above the optimum velocity, within the range investigated, the mass transfer was shown to be independent of the overall fluidization velocity [33]. This result supports the statement that gas-convection heat and mass transfer depend on u_{mf}, as discussed in App C.

4.2. Particle convection

Increase of the fluidization velocity above u_{mf} forms bubbles whose motion agitates the bed. The higher the velocity, the more agitation. The stirred bed particles are moved to a heat transfer surface in the form of "packets", bringing heat to or from the surface. The mechanism occurs in a similar form in the transfer between particles of different sizes, between inert bed particles and active particles or vice versa. The smaller the active particle, the more effective is the transfer of heat because of the shorter particle contact-time that does not significantly affect the temperature difference between the active particle and its surrounding. This tends to increase the heat transfer between the particles. However, when the size of the active particles approaches the small (bed) particle size, and d_a tends to d_i, the heat transfer mechanism disappears or is reduced beause the particles move together. Measurements (Prins [34]) show that the impact of the change of size of the active particle is less important for large active particles. This is most likely related to the residence length of a packet on the surface of an active particle becoming shorter than the size of a large particle, "the large particle" limit [35] is reached.

The particle convection increases when the velocity changes from u_{mf} to u_{opt}, where the maximum particle-convection heat transfer is attained. Prins [34] compared the transfer to both moving and fixed active particles in a bed and came to the conclusion that the difference between the *Nu* values in these two cases under otherwise similar conditions was less than 10%. The measured heat transfer coefficients (HTC) to a 15 mm graphite sphere [34] illustrates the variation of heat transfer, while using several (inert) bed particle sizes, Fig. 5.

The total HTCs from the B&P model do not vary with velocity, and furthermore, they are a little higher than Prins's measured values.

Fig. 5 treats a large active particle. In addition, Prins [34] identified maxima of active particles with sizes down to 4 mm and presented the results in the form of correlations. Fig. 6 corresponds to Fig. 5 (15 mm active particles) and compares the maxima from Prins [34] and Baskakov et al. [23]. The maxima coincide reasonably well with those derived from Eq. (5). The same small discrepancy is noted for larger inert particles on Fig. 7 in a plot of the HTC as a function of the active particle size for two bed particle-sizes, comparing with the B&P model. Prins's maximum heat transfer data cover several sizes of active particles in the range 4 to 15 mm, Fig. 7, whereas Baskakov's value is a single extreme coefficient.

The agreement is sufficiently good to prove that *Nu* values resulting from the B&P model, $Nu_{max,a}$, are maxima for active particle sizes in the range from $d_a = d_i$ until the "large active particle" (index *a* in $Nu_{max,a}$

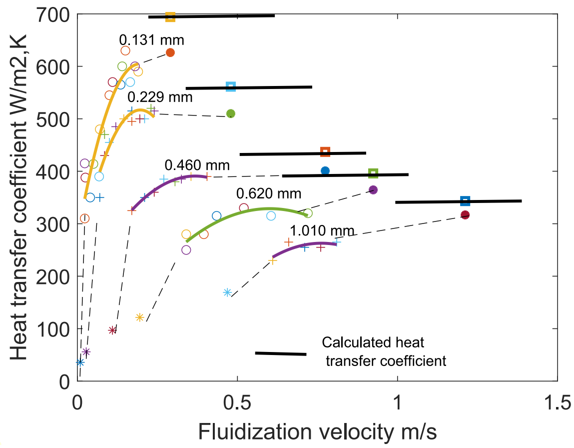

Fig. 5. Prins's measured data [34] (o, +) and fitted, thick curves for an active particle (15 mm) in beds of smaller inert particles (5 cases, whose particle sizes are indicated on the curves). Connected (with dashed lines) data at u_{mf} and u_{opt} from Baskakov et al. [23] max HTC from Eq. (5, both terms), Baskakov&Suprun [22], and Čatipović [24] (*). Resulting HTCs from the B&P model are marked with horizontal lines to indicate the lack of dependence on velocity.

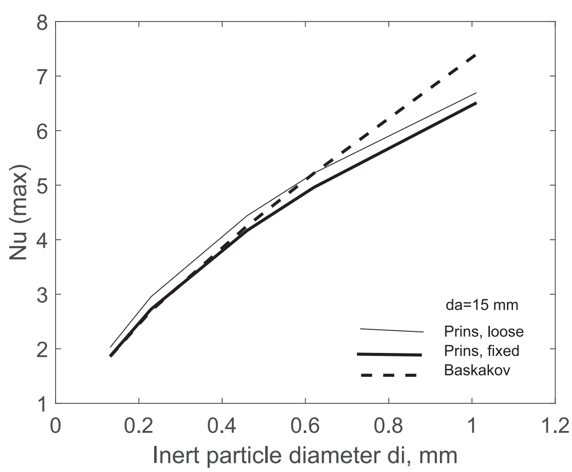

Fig. 6. Nu_{max} for a 15 mm spherical particle, in beds of d_i particles. Comparison between Prins's data [34] for fixed and loose active spheres (solid lines) and the correlation of Baskakov et al. [23] (dashed line, Eq. 5).

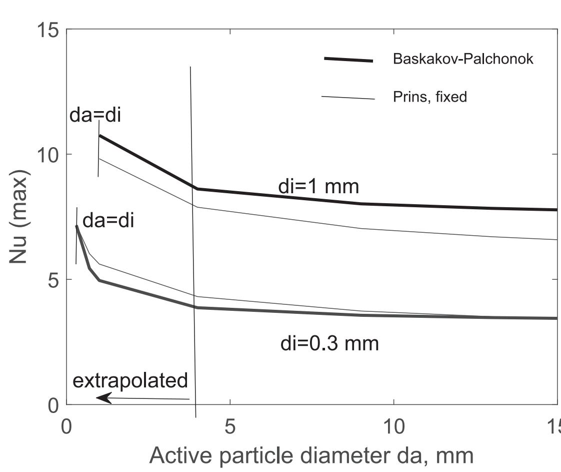

Fig. 7. $Nu_{max,a}$ for fixed and loose active particles of size d_a, calculated with Prins's correlation [34], compared with values from the B&P model.

relates to a certain active particle size d_a, different from the large active particles in Ref [23], Nu_{max}).

In the B&P model there is an increasing contribution from conduction as d_a approaches d_i. The smallest active particle treated by Prins, $d_a = 4$ mm, is large enough to assume that the contribution of conduction is still not important for Nu_i. Also, Figs. 6 and 7 show that the difference between fixed and loose active particles is about the same for all d_a. It does not increase when d_a approaches d_i, which could be imagined, because, the smaller the active particles are, the more they are carried around by the surrounding bed particles. Then, the relative velocity between neighbouring particle declines, and so should the particle-induced heat transfer. However, Prins's measurements do not confirm this.

The heat transfer maxima occur at certain velocities, the optimum velocities, $u_{opt(a)}$. The uncertainty of the optimum velocities is greater than that of $Nu_{max,a}$, as seen from Fig. 8, compared with Figs. 6 and 7. Shah [36] states that the correlation for optimum velocity, Eq. (7) [26] "was found to be in good agreement with data". Prins's data, read from diagrams of heat transfer maxima in his thesis, shown in Fig. 8, are clearly below Eq, (7) even in the 15 mm case. A tentative explanation for this deviation is that the locations of the maxima are incertain because of the wide extension of a maximum and the scatter in the measured data points. As seen in Figs. 5 and 10, the locations of the maxima could have been better determined if the measurements had included higher velocities. Another tentative explanation is that the data on Fig. 8 are correct, and that the optimum velocity depands on the size of the active particle. This effect has not been shown clearly in the literature, in which most data are from large particles or surfaces where undoubtedly Eq. (7) is valid. More and systematic data are needed to validate the variation of the optimum velocity for small active particles.

4.3. Estimation of heat transfer at velocities between u_{mf} and u_{opt}

Prins's data set (especially the values shown on Fig. 5) has been widely used for comparison with modelling results, starting with Agarwal [37], who used a developed form of the packet model, requiring information on the thermal conductivity of a packet and the times of descent and acsent of an active particle in the bed when it is not in a bubble. The gas convection was modelled using Agarwal's work on mass transfer. The model was applied to the 15 mm particle of Prins, and the agreement is reasonable within error bounds of ±15%, with tendencies of values both above and below the measured data. This work was followed by a study of Chao et al. [38], supported by their own measurements of the surface resistence to heat transfer and the mean emulsion residence time, applying the packet model. Finally, von Berg et al. [39]

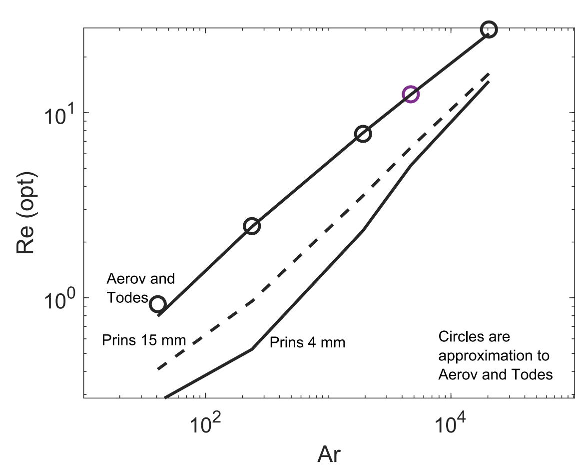

Fig. 8. Optimum velocities from Aerov and Todes's correlation, Eq. (7), and from Prins data [34] for $d_a = 15$ and 4 mm active particles. The circles are an approximative representation of Eq. (7), Eq. (7a).

analyzed existing model results, including the results from Prins's 15 mm particle. The works mentioned that the max values of Baskakov et al. [23] or the B&P model do not resolve the velocity between u_{mf} and u_{opt} as indicated in Fig. 5, although the agreement of the maximum values was deemed to be reasonable.

For a simplified description of the velocity dependency in the range between u_{opt} and u_{mf}, the data of Prins, shown on Fig. 5, can be used to provide a power-law correlation, thus avoiding the complexity of the packet model and its requirement of input data. To describe the character of the data in a consistent way, Prins's measured optimum velocities and maximum HTCs were used, as illustrated on Figs. 6 and 7, rather than the values inserted in Fig. 5, taken from other sources.

The velocity variations in the HTC are caused by the particles' movements. Therefore the gas convection HTCs should be subtracted, leaving only the part affected by particles for the comparison with the first term of Eq. (5), Nu_{max} - Nu_{gc}. This formulation results in the dimensionless curves in Fig. 9, with the data from Fig. 5, showing a dependency of the particle convection with a power of 0.2, as expressed in a function $f(Re)$ by Eq. (10) from Fig. 9. With $f(Re)$, the resulting Nu in Eq. (9) can be written,

$$Nu = Nu_{gc} + \left(Nu_{max,a} - Nu_{gc}\right) f(Re) \tag{9}$$

$$f(Re) = \left(\left(Re - Re_{mf}\right) / \left(Re_{opt} - Re_{mf}\right)\right)^{0.2} \tag{10}$$

Nu_{gc} is the last part of Eq. (5), the gas-convection component. $Nu_{max,a} = h_{max}(d_a, d_i)\, d_i / k_g$ is the value calculated by the B&P model for d_a and d_i. The term ($Nu_{max,a}$ - Nu_{gc}) is the particle-convection component for $Re = u d_i \rho_g / \mu$. A corresponding description can be given for the related optimum velocities, either by Eq. (7) or by a correlation for Prins's max values, (in this case of $d_a = 4$ mm particles),

$$Re_{opt} = 0.02 Ar^{0.65} \tag{11}$$

Prins's data for $d_a = 4$ mm could be used as an example of the application of the correlation Eqs. (9, 10). This is presented in Fig. 10. As seen in Figs. 5 and 10, there is a certain scatter in Prins's data points around the resulting curves, but this is within the error bounds of the original data. There are no systematic trends within the range of data, $0.131 \le d_i \le 1.010$ mm.

Figs. 6, 7, and 10 show that Nu_{max} according to Baskakov et al. [23] and Prins's correlation together with the power law agree quite well also for active particles smaller than the "large" size, so this fitted power-law expression can be used in all cases. However, the optimum velocities are not well represented by the correlation of Aerov and Todes [26], as

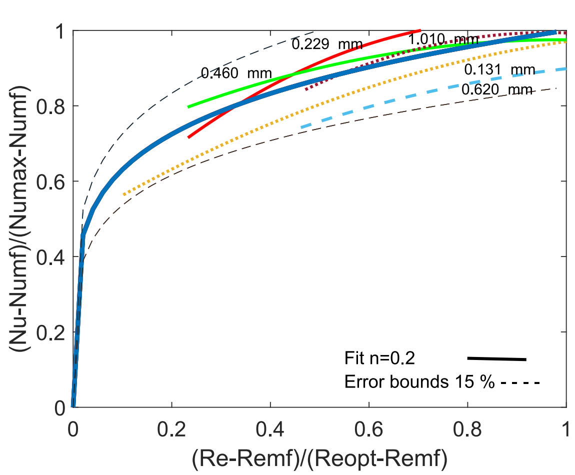

Fig. 9. The data of Fig. 5 plotted in dimensionless form with u_{opt} and Nu_{max} as measured by Prins [34]. The approximation by a power law with $n = 0.2$ is shown with a thick curve.

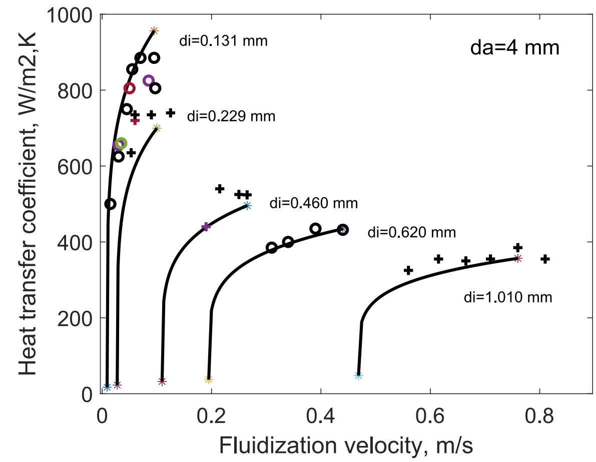

Fig. 10. Fluidization velocities from Prins's data, measured points from $d_a = 4$ mm [34]. Curves according to Eqs. (9) and (10) with $Nu_{max,a}$ according to B&P, and Re_{mf} and Nu_{gc} according to [22,24]. Re_{opt} is taken from Prins's diagram [34], Eq. (11).

shown in Fig. 8, and the actual measured data were used in the diagram of Fig. 10.

4.4. Influence of velocity on heat transfer at $u > u_{opt}$

Figs. (9, 10) represent one part of the velocity dependence, the rising heat transfer during an increase of velocity from u_{mf} to u_{opt}. Increase of velocity above u_{opt} tends to further agitation and dilution of the bed because of increased bubbling, although the dilution may be reduced by through-flow of gas through the bubbles. The structure of the particle phase, discussed in connection to Fig. 2, remains dependent on u_{mf}. A consequence of the dilution should be a decline of the effective particle convection, at least for small bed particles, while for larger (mm-size) bed particles the gas convection plays a greater role, and the decline of the particle convection is less significant for the total HTC. The region of fluidization of $u > u_{opt}$ has not been thoroughly studied, and the recommendations for heat transfer are simplified, although modelling has been carried out [41,42,44]. The measurements presented for this region are uncertain to interpret and show either a declining or a constant heat transfer, for instance, in [34,40–44]. High velocity makes the data even more complicated to interpret because, while the gas velocity increases, the bed ceases to be a unit of investigation but becomes a component in a circulating system (CFB) where the regime of fluidization may change depending on bed particle-size (the group according to Geldart) and vessel dimensions (slugging vs non-slugging beds with Group B particles). Recognizing that more consistent data are needed, a tentative approach could be proposed: the change in the post-optimum particle-convective heat-transfer (Nu_{pc}) is assumed to be proportional to the change in the particle concentration in the bed, whereas the gas-convective heat-transfer (Nu_{gc}) remains dependent on u_{mf}, such as shown in App C, $Nu_{pc} = Nu$ - Nu_{gc}, or $Nu_{pc,max} = Nu_{max}$ - Nu_{gc} is the particle-convective heat-transfer. At $u > u_{opt}$ the increase in velocity results in a decay of heat transfer, which is assumed to be proportional to the change of voidage, $d\varepsilon/du$,

$$Nu_{pc} = Nu_{pc,max} - Nu_{pc,max}\left(d\varepsilon/du\right)\left(u - u_{opt}\right) \tag{12}$$

Measurements from bottom beds of circulating fluidized bed (CFB) boilers [45,46] give a simple picture, Fig. 11, yielding $d\varepsilon/du = 0.022$ in the size range of bed particles of 0.28 to 0.43 mm (ash or silica sand). The beds operate with fluidization velocities up to around 6 m/s. Still, the bed expansion is moderate. This is explained by the bubbling character of these non-slugging beds [3] with a considerable gas through-flow through the bubbles. It also depends on the conditions for

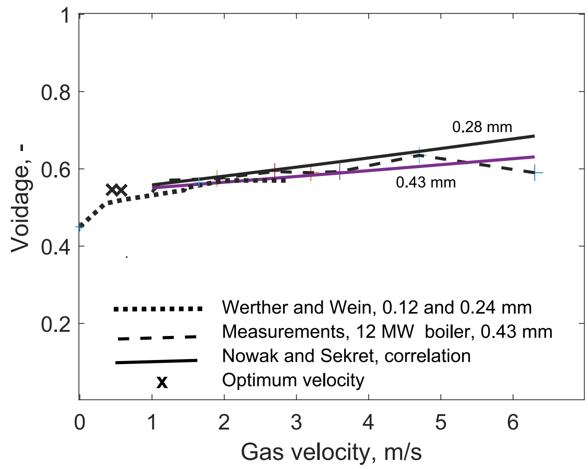

Fig. 11. Voidage of the particle phase from Fig. 2 compared with the bed voidage in the part of the bed with constant pressure drop (below the splash zone), measured in the 12 MW CFB boiler at Chalmers University [45] and in a 670 MW CFB boiler [46]. The crosses mark the optimum velocities for the bed materials of 0.28 and 0.43 mm, respectively.

measurement: the data are recorded in the part of the bed having constant pressure drop with height (as in all bubbling beds). Above this part of the bed, the pressure drop declines with height in a non-linear way in the fluctuating surface region and in the splash zone of the bed. When the velocity increases, the pressure drop changes very little (as seen in Fig. 11), but the height of the dense bed decreases while more bed material moves into the splash and transport zones of the riser. The total riser pressure-drop is usually kept constant by removal or addition of bed material [45,46].

This evaluation concerns the dense bottom bed of a CFB system where the B&P model can be applied. In the CFB system, also active particles are elutriated from the dense bottom bed together with inert particles and travel upwards in the splash and transport zones where the particle suspension is not dense, $\varepsilon \rightarrow 1$, This means that they can be described approximately by heat and mass transfer relationships simillar to those of single-phase flow with a conduction term equal to 2 and a particle *Re* number based on the slip velocity (the velocity experienced by a moving particle).

5. Summary of the results

The approach called the Baskakov-Palchonok model (in short, B&P model) is described and analyzed in [4]. It determines heat and mass transfer coefficients, expressed as *Nu* or *Sh* by interpolation between two limiting cases $d_i = d_a$ (index 1) and large d_a (index ∞), by a function $f = (d_i/d_a)^{0.66}$ [5]. Baskakov et al. [35] proposed an exponential interpolation function.

In the model, the relationships are expressed in the form of *Ar*. Here, *Ar* is changed into *Re*. The impacts of assumptions and approximations related to the change from *Ar* to *Re* are small in view of the uncertainties in *Nu* and *Sh* found by comparing various investigations [4].

$$Nu_i = Nu_{i,\infty} + (Nu_1 - Nu_{i,\infty})f(d_i/d_a) \tag{13}$$

$$Sh_i = Sh_{i,\infty} + (Sh_1 - Sh_{i,\infty})f(d_i/d_a) \tag{14}$$

The $d_a = d_i$ limit, introduced in Eqs. (13, 14) with Re_{mf} from Eq. (4), is.

$$Nu_1 = Nu_0 + \left[6.73\mathrm{Re}_{mf} + 0.10\mathrm{Re}_{mf}^2\right]^{0.39} Pr^{0.33} \tag{1a}$$

$$Sh_1 = 2\varepsilon_{mf} + \left[6.73\mathrm{Re}_{mf} + 0.10\mathrm{Re}_{mf}^2\right]^{0.39} Sc^{0.33} \tag{2a}$$

The large particle limit, $d_a >> d_i$, introduced in Eqs. (13, 14) with Re_{opt} from Eq. (7), is.

$$Nu_{i,\infty} = 1.64\, Re_{i,\,opt}{}^{0.40} + \left(156.5\, Re_{i,mf} + 2.3\, Re_{i,mf}{}^2\right)^{0.5} Pr^{0.33} \tag{5b}$$

$$Sh_{i,\infty} = 2\varepsilon\, d_i \big/ d_a + \left(127.8\, Re_{i,m\,f} + 1.9\, Re_{i,\,mf}{}^2\right)^{0.5} Sc^{0.33} \tag{6c}$$

Eqs. (2a, 6c) inserted into Eq. (14) gives the mass transfer result.

To evaluate the influence of velocity on the particle-convective component of heat transfer, additional treatment is required for $u_{mf} \le u \le u_{opt}$. and for $u > u_{opt}$. The heat transfer result of Eq. (13) for a certain d_a is called $Nu_i = Nu_{max,a}$, different from $Nu_{i,\infty}$, the maximum for $d_a >> d_i$. Eqs. (9, 10) are valid at velocities between u_{mf} and u_{opt},

$$Nu = Nu_{gc} + \left(Nu_{max,a} - Nu_{gc}\right) f\,(Re) \tag{9}$$

$$f\,(Re) = \left(\left(Re - Re_{mf}\right) / \left(Re_{opt} - Re_{mf}\right)\right)^{0.2} \tag{10}$$

At fluidization velocities above u_{opt}, $Nu_{pc} = Nu - Nu_{gc}$, or $Nu_{pc,max} = Nu_{max,a} - Nu_{gc}$ is the particle-convective heat-transfer, where Nu_{gc} is the gas-convection heat-transfer from Eq. (5).

The change of heat transfer with velocity can be written with $d\varepsilon/du = 0.022$ as,

$$Nu_{pc} = Nu_{pc,max}\,\left(1 - d\varepsilon/du\,\left(u - u_{opt}\right)\right) \tag{12}$$

6. Application for $u_{mf} \le u \le u_{opt}$ and $u >> u_{opt}$

Wunder, quoted by Martin [41], presented a series of measurements of the heat transfer coefficient vs. velocity for several bed material sizes. Here, glass beads of 265 or 400 μm, are selected as bed materials for comparison with calculations by the equations listed in §5. The active "particle" was a vertical cylinder of 0.040 m diameter and 0.280 m long, clearly $d_a >> d_i$ and $Nu_{max,a} = Nu_{i,\infty}$. The bed diameter was 0.200 m and the height 0.500 m, as estimated from Martin [41] and Wunder and Mersmann [47].

The general features of the measurements is captured by the calculation procedure as seen in Fig. 12, but the discrepancies are obvious and will be further discussed below.

7. Discussion

The computational scheme is based on fitting to measurements. It is intended to be applied primarily in commercial fluidized-bed converters of solid fuels (boilers and gasifiers). Because of the fitting to measurements, the results are correspondingly limited, but slightly generalized by the use of dimensionless quantities.

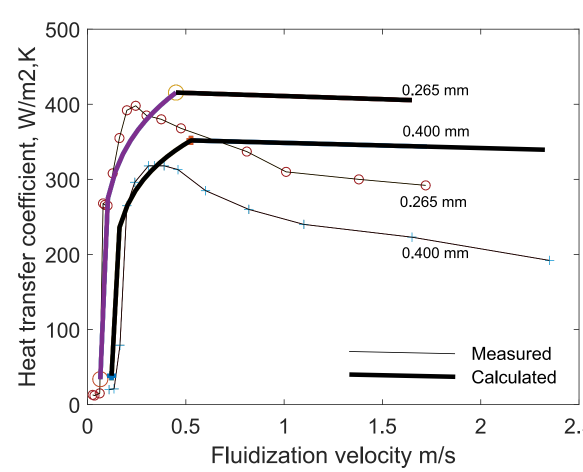

Fig. 12. Comparison between calculation by Eq. (12) with dε/du = 0.022 and Wunder's measurements obtained from [41].

The comparison in Fig. 12, presented at the same temperature as used by Wunder (298 K), reveals several discrepancies. They are related to 1) the maximum heat transfer 2) the corresponding optimum velocity, and 3) the decay in HTC at super-optimum velocities (Eq. 12). Di Natale et al. [43, Fig. 2] investigated active particles (heat-exchange surfaces) of various shapes in a 0.1 m diameter test tube with a set of bed-material sizes. Their figure of interest here used corundum particles of a size of 310 μm. They found that there was a considerable variation in heat-transfer results depending on the form of the heat-transfer surface. Spheres had a higher HTC than vertical cylinders. In all cases the HTC was about constant with velocity from u_{opt} to up to the final value $u = 2u_{opt}$. Wunder and Mersmann [47, Fig. 1] compared the HTC to a probe like the one used by Wunder in Fig. 12 in beds with different widths (0.080, 0.200, and 0.690 m) using glass spheres of 200 μm diameter as a bed material. They observed significant differences in the three beds in the three items mentioned above: the maximum heat transfer and the related optimum velocity depended on the width of the beds, highest in the wide bed and smallest in the narrow bed. Above u_{opt}, the HTC decayed moderately with velocity in all beds, but in different ways.

In the present example of bottom beds in commercial CFB devices the HTC changes very little in the $u > u_{opt}$ region up to a very high velocity, as seen in Fig. 11 and then in Fig. 12. There are no similar data for comparison. The data available are from laboratory-scale vessels, whose size results in transition of fluidisation regimes during an incerease in velocity: from bubbling to slugging, turbulent, and fast fluidization. Sometimes the regimes of fluidization are taken into account, but in most cases nothing is mentioned about the state of fluidization. In some results, the HTC-velocity relationship falls with increasing velocity, in others it is fairly constant, even in the case of Group A paricles [44]. In short, the available data cover just a few times the u_{opt} and they tend in various directions (constant or falling) without much explanation, perhhaps a result of the interaction with the walls of the fluidization vessel. This is a topic worth further systematic study. Heat transfer data from CFBs are needed to validate the performance at high velocity, such as seen in Fig. 12. Finally, it can be concluded that the transformation from Ar to Re is not responsible for the discrepances observed.

8. Conclusions

The model for the calculation of *Nu* and *Sh* is summarized in §5. The correlations of *Nu* or *Sh* as a function of *Ar* are translated into *Re*, but the velocities in *Re* are those of u_{mf} and u_{opt}, so they are related to d_i, just like *Ar,* and they are not free functions of the superficial velocity *u*. Nevertheless, some conclusions regarding the dependency on velocity can be drawn. At $d_a = d_i$ the heat and mass transfer takes place in the particle phase at a velocity of u_{mf}, related to the bed-particle size (d_i), independent of the fluidization velocity *u*. The same is true about the gas-convection terms, whether they are included in the optimum velocity or not; they are related to u_{mf}. The velocity dependency of heat transfer is mostly conected to the particle phase and its movement (caused by bubbles) and the related voidage, while the mass is transferred (*Sh*) in the particle phase of the bed at u_{mf}, it is described by Eqs. (2, 6b).

The conduction/diffusion transfer is important when $d_a \approx d_i$, but it becomes insignificant when *Nu* is related to d_i if $d_a >> d_i$, as explained by Eq. (B8).

The radiation component of heat transfer can be added, but this is not done here, focussing on conduction/diffusion and convection.

Additional relationships are needed in the case of heat transfer to describe the velocity variation around u_{opt}. The present approach is based on measurements, and this leads to empirical relationships. In the literature, one can find modelling approaches. However, the modelling also relies on measurements.

The particle-convection term of heat transfer is strongly related to the movements of the bed, caused by changes in the fluidization velocity between u_{mf} and u_{opt}. At velocities above u_{opt}, the total transfer conditions are relatively constant, at least for larger bed-particle sizes, because of the influence of gas convection. In this velocity region, the particle-convective heat-transfer tends to decline because the bed is becoming diluted. However, there are several factors mitigating this tendency: in addition to the constant gas convection (for large bed particles), the gas through-flow through the bubbles reduces the bed expansion. In such cases the particle density of the bed remains without large changes with velocity as long as there is a bed. Published measurment results give the impression that the knowledge on this region is not well established; often investigations do not consider wall and system effects.

CRediT authorship contribution statement

Bo Leckner: Writing – review & editing, Writing – original draft, Visualization, Validation, Software, Resources, Project administration, Methodology, Investigation, Formal analysis, Data curation, Conceptualization.

Declaration of competing interest

There are no interests to declare.

Appendix A. The conduction term

Heat transfer in a fluidized bed depends on conduction, gas and particle convection, and radiation. At low temperature and small bed particles conduction dominates. At higher temperatures radiation heat transfer can be added. The present derivation is made for equally sized, small ($d_i < 1$ mm) bed particles. One particle, an active particle, of size d_a and temperature T_a, exchanges heat with the surrounding particles (of size d_i and of temperature T_i), under the assumption of an even voidage ε over the entire surrounding space. The heat transfer by steady state conduction across a spherical surface ($R_a = d_a/2$ and in the range $R_a < R < R_+$) is.

$$Q = \pi {d_a}^2\, k_g\, (dT/dR)_{R=Ra} \tag{A1}$$

The derivative of the temperature is taken on the gas side, just outside of the surface of the active particle. An active particle is surrounded by inert bed particles, but most of the surface of the active particle (at R_a) is in contact with gas, whose thermal conductivity is k_g.

The heat flow can also be expressed by the definition of the heat-transfer coefficient, *h*,

$$Q = \pi {d_a}^2 h (T_a - T_i) \tag{A2}$$

Eqs. (A1, A2) give the same *Q*. After integration between $R = R_a$ ($d_a/2$) and a fictitious spherical surface with radius R_+ ($d_+/2$),

$$h\pi d_a^2 (T_a - T_i) = \frac{2\pi k_g (T_a - T_i)}{1/d_a - 1/d_+} \tag{A3}$$

Extending the outer integration limit to the entire space ($d_+ \rightarrow \infty$) yields the well-known single-phase result,

$$Nu_a = hd_a/k_g = 2 \tag{A4}$$

In the case of a particle in a fluidized bed, the integration cannot be carried to infinity like in single-phase flow, but only up to a certain distance R_+ from the particle surface, and the contribution of the surrounding inert particles of size d_i, should be considered [27], p. 523. Then Eq. (A3) gives the conductive component of heat transfer to the active particle.

$$Nu_{a,0} = \frac{2}{1 - d_a/d_+} \text{ where } \frac{\pi d_a^3/6}{\pi d_+^3/6} = (1 - \varepsilon_+) \tag{A5}$$

(1-ε_+) is the particle volume concentration in the bed around the active particle. With the voidage ε_+, Eq. (A5) can be written,

$$Nu_{a,0} = \frac{2}{\left(1 - (1 - \varepsilon_+)^{1/3}\right)} \tag{A6}$$

This is based on the assumption that the surface of the active particle is in contact with gas (boundary condition of Eq. A1). An alternative assumption would be that the particle is surrounded by a particle suspension with an effective thermal conductivity k_{eff}, valid in the entire particle suspension up to the surface of the active particle. For simplicity, the surrounding particle-suspension is assumed to have a constant temperature T_i and a constant voidage ε_+. Then, again the integration of Eqs. (A1, A2) can be carried out to infinity under the assumption that k_{eff} is valid in the entire field. If the definition of the Nusselt number is maintained and related to the thermal conductivity of the gas k_g, the result becomes.

$$Nu_{a,0} = 2\cdot(k_{eff}/k_g) \tag{A7}$$

From Ofuchi and Kunii [31] and Yagi and Kunii [48] k_{eff}/k_g are estimated to between 4 and 6, which would result in an $Nu_{a,0}$ of the same magnitude as the one of Eq. (A6). However, one complication is noted [31]: a particle layer close to a vertical wall has a greater voidage and lower thermal conductivity than the rest of the particle suspension, and that influences locally the ratio k_{eff}/k_g. The impact of this irregularity on an active particle of the same size as the surrounding inert particles is unknown, but it seems reasonable that the active particle is exposed to the same conditions as the rest of the particle bed, which results in higher k_{eff}/k_g ratio than at a vertical wall. For a sand bed, this gives a ratio of about 8, assumed here to be representative for a bed in a fuel converter. This can be compared with the independent estimation of Decker and Glicksman [49] who give an indicative value of $Nu_{a,0} = 12$ for a spherical particle of normal roughness. More irregular particles may have half that value. The assumptions and the data obtained are rather coarse, but one conclusion is firm: $Nu_{a,0}$ is greater than 2 because of the enhancement of conduction by the neighbouring particles, having a thermal conductivity greater than that of the surrounding gas.

As seen from the derivation of Eqs. (A3, A4) $Nu_{a,0}$ is related to the size of the active particle d_a. In the case of $d_a = d_i$, the size is also d_i. In large active particle cases d_i is usually the characteristic dimension of Nu. Hence, in the large active particle cases a transformation,

$$Nu_{i,0} = Nu_{a,0}\, d_i/d_a \tag{A8}$$

makes $Nu_{i,0}$ (d_i) insignificant when $d_a >> d_i$. Therefore, it is not included in the relationships in a large active particle case.

Appendix B. The relation between *Ar* and *Re* at minimum fluidization

Ergun [20], based on his own and previous data, determined coefficients of an expression for the pressure drop ΔP from a gas flow through a packed particle-bed of height ΔH, using the conventional relationship for flow in a channel through the bed

$$\Delta P = \xi\left(\frac{\rho_g v^2}{2}\right)\frac{\Delta H}{D_h} \tag{B1}$$

where ξ is the drag coefficient, $v = u/\varepsilon_{pb}$ is the local gas velocity, $D_h = \frac{2}{3}\frac{\varepsilon_{pb}}{1-\varepsilon_{pb}}d_i$ the hydraulic diameter of the channel, ε_{pb} the voidage of the packed bed, and d_i the size of the particles. With the drag coefficient (the term in brackets of Eq. B2) determined for a packed bed, the Ergun equation, now expressed in terms of superficial velocity u, gives the pressure drop ΔP across the bed height ΔH

$$\Delta P = \left[150\frac{1-\varepsilon_{pb}}{\mathrm{Re}mf} + 1.75\right]\frac{\rho_g u^2}{d_i}\frac{1-\varepsilon_{pb}}{\varepsilon_{pb}^3}\Delta H \tag{B2}$$

The gravity causes an opposite force, the weight, acting on the particle layer ΔH,

$$F_g = g(1-\varepsilon_{pb})(\rho_i - \rho_g)\Delta H \tag{B3}$$

where ρ_i and ρ_g are the particle and gas densities, and g is the acceleration of gravity. When the gas velocity increases, the two forces eventually become equal in the minimum fluidization condition (index mf). With $Ar = \frac{d_i^3(\rho_i-\rho_g)\rho_g g}{\mu^2}$, $\mathrm{Re} = \frac{d_i u \rho_g}{\mu}$, $\varepsilon = \varepsilon_{mf}$, and $u = u_{mf}$, Eqs. (B2, B3) yield

$$Ar = 150C_2Re_{mf} + 1.75C_1Re_{mf}^2 \tag{B4}$$

A sphericity factor φ accounts for deviations from a spherical shape,

$$C_1 = \frac{1}{\varphi\varepsilon_{mf}^3} \text{ and } C_2 = \frac{1-\varepsilon_{mf}}{\varphi^2\varepsilon_{mf}^3} \tag{B5}$$

This form of the Ergun equation serves as a basis for several correlations to determine the minimum fluidization velocity u_{mf}, contained in Re_{mf}. The correlations include the coefficients C_1 and C_2 with the voidage and sphericity, given by experimental data. The agreement between similar correlations is far from good. The reason is the uncertainty in characterizing the shape of a particle in the form of a sphericity factor, and furthermore, particle size and size distribution influence the voidage. For the present purpose it is sufficient to choose the most common correlation, that of Wen and Yu [21], even if deviations are found [50]. Then, Eqs. (B4, B5) with $C_1 \approx 14$ and $C_2 \approx 11$ from [21] become.

$$Ar = 1650\mathrm{Re}_{mf} + 24.5\mathrm{Re}_{mf}^2 \text{ or } \mathrm{Re}_{mf} = -33.7 + \sqrt{33.7^2 + 0.0408Ar} \tag{B6}$$

This derivation is valid for Group A and B particles where the drag and gravity forces dominate.

Appendix C. The gas convective constituent

Baskakov and Suprun [22] measured diffusion of gas from naphthalene cylinders immersed in a fluidized bed, giving a correlation in *Sh*. Referring to the analogy between heat and mass transfer, this gas-convective mass-transfer term could be translated to gas-convection heat-transfer without interference from particle-convective heat-transfer,

$$Sh = Nu\,(Sc/Pr)^{0.33} \tag{C1}$$

With the media used [22],

$$(Pr/Sc)^{0.33} = (D/a)^{0.33} = 0.7 \tag{C2}$$

where D is mass diffusivity and a thermal diffusivity. The correlation obtained

$$Nu_{i,gc} = 0.0175Ar^{0.46}Pr^{0.33} \tag{C3}$$

was later replotted and fitted to more results [23], yielding the updated correlation,

$$Nu_{i,gc} = 0.009Ar^{0.5}\,Pr^{0.33} \tag{C4}$$

According to Eqs. (C1 and C2), the corresponding mass-transfer relationship is

$$Sh = 0.006Ar^{0.5}\,Sc^{0.33} \tag{C5}$$

where the coefficient is obtained as $0.006 \approx 0.009{\cdot}0.7$. Because of a presumed printing error, the coefficients were interchanged in a following paper, Baskakov et al. [35], and that has affected some quoting publications. Fortunately, the difference between the coefficients is small, and the error following the use of the erroneous coefficients is not important.

Baskakov and Suprun [22] presented basic results in a diagram, which could be expanded, correcting Eq. (C3) by $(u/u_{opt})^{0.3}$ for velocities below u_{opt}, as proposed by the authors. The symbols (o and +) in Fig. C1 indicate heat transfer at the optimum and minimum velocities.

The diagram shows heat-transfer coefficients at velocities above the optimum ones (transformed from measured mass-transfer coefficients), forming horizontal lines.

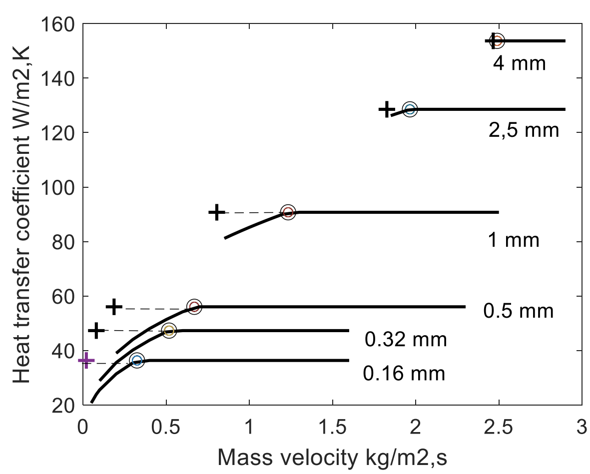

Fig. C1. Gas convective heat transfer in fluidized bed [22, Fig. 2]. The diagram is calculated by Eq. (C3) with Ar from Eq. (4), completed with a $(u/u_{opt})^{0.3}$ correction at velocities below the optimum one.

The diagram shows curves for bed-particle sizes. Dashed lines are extrapolations from u_{opt} (o) to u_{mf} (+). The temperature used of about 330 K gives a gas density of around 1, so the horizontal scale is about the same in m/s. The following relationships were used:

$$Re_{mf} = -33.7 + \mathrm{sqrt}\left(33.7^2 + 0.0408Ar\right) \tag{C6}$$

$$Ar_{mf} = 1650Re_{mf} + 24.5{Re_{mf}}^2 \tag{C7}$$

$$h = \left(k_g/d_i\right)\,0.0175\,{Ar_{mf}}^{0.46}Pr^{0.33} \tag{C8}$$

The velocities u_{mf} and u_{opt} are calculated from Eqs. (4) and (7).

Two velocities should be considered when interpreting the results. One is the total fluidization velocity marked on the horizontal scale. The other velocity is u_{mf} prevailing in the particle phase and dependent on bed-particle size. The horizontal heat-transfer relationships do not depend on the fluidization velocity of the bed. Only at total fluidization velocities below the optimum one, a decay in heat transfer with velocity was observed and described in [22] by the velocity correction $(u/u_{opt})^{0.3}$, introduced in Fig. C1. The lack of influence of the total velocity in most part of the curves can be understood from the fact that the particles are contained in the particle phase, subject to a velocity u_{mf}, In the low limit of velocities, the total fluidization velocity reaches $u = u_{mf}$, marked with a cross in the diagram and calculated by Eq. (C3), connected to the curves by the dashed lines. At velocities below u_{mf}, the bed turns into a packed bed. The distance between u_{mf} and u_{opt} becomes smaller as the particle size (Ar) increases, just as it should according to Fig. 1. The coincidence between the measured heat transfer coefficients of Baskakov and Suprun and those calculated with Eq. (C3) with Ar_{mf} from Eq. (4) and the independence of these values from the total superficial fluidization velocity support the assumption that the active particles are subjected to gas-convection heat-transfer in the particle phase. The validity of the independence of the fluidization velocity of Eq. (C3) all the way down to the fluidization velocity u_{mf} (the +) is further supported by the results of Čatipović [24] (Fig. 3), who did not acount for any reduction of heat transfer by a velocity correction close to u_{mf}. The velocity correction, $(u/u_{opt})^{0.3}$, is not well motivated in the original publication [22], but it is kept in Fig. C1 anyway for historic reasons. Moreover, there is no correction for the influence of bubbles in these data.

Data availability

No data was used for the research described in the article.

References

[1] J.R. Grace, Fluidized bed reactors, chapter 17.1, in: E. Michaelides, C.L. Crowe, J. D. Schwartzkopf (Eds.), Multiphase Flow Handbook, CRC Press, Boca Raton, 2016.
[2] T. Wytrwat, E.-U. Hartge, M. Yazdanpanah, S. Heinrich, Influences on the transition from bubbling to turbulent fluidization for Geldart's group B particles, Powder Technol. 375 (2020) 81–88.
[3] B. Leckner, Fluidization characteristics of circulating fluidized bed boilers, Chem. Ing. Tech. 95 (2023) 1–9.
[4] B. Leckner, Heat and mass transfer to/from active particles in a fluidized bed—an analysis of the Baskakov-Palchonok correlation, Int. J. Heat Mass Transf. 168 (2021) 120860.
[5] G.I. Palchonok, Heat and Mass Transfer to a Single Particle in a Fluidized Bed, Dr Thesis, Chalmers University of Technology, Göteborg, Sweden, 1998.
[6] G.I. Palchonok, A.F. Dolidovich, S. Andersson, B. Leckner, Calculation of True Heat and Mass Transfer Coefficients Between Particles and a Fluidized Bed, Fluidization VII, Eng. Found, 1992, pp. 913–920.
[7] M.M. Avedesian, J.F. Davidson, Combustion of carbon particles in a fluidized bed, Trans. Inst. Chem. Eng. 51 (1973) 121–131.
[8] A.R. Abrahamsen, D. Geldart, Behaviour of gas-fluidized beds of fine powders part II. Voidage of the dense phase in bubbling beds, Powder Technol. 26 (1980) 47–55.
[9] H.T. Bi, P.-C. Su, Local phase holdups in gas-solids fluidization and transport, AICHE J. 47 (2001) 2025–2031.
[10] D. Geldart, Expansion of gas fluidized beds, Ind. Eng. Chem. Res. 43 (2004) 5802–5809.
[11] J. Baeyens, S.Y. Wu, Bed expansion and the visible bubble flow rate in gas fluidized beds, Adv. Powder Technol. 3 (1992) 163–189.
[12] I.A. Khattab, C. Kuroda, M. Ishida, Radial and vertical distributions of gas the interstitial gas velocity in a fluidized bed, J. Chem. Eng. Japan 21 (1988) 282–287.
[13] P.N. Rowe, C.X.R. Yacono, The bubbling behaviour of fine powders when fluidized, Chem. Eng. Sci. 31 (1976) 1179–1192.
[14] J.S. Harlow, P. Nicoletti, Observations of fluidized bed coalescence using capacitance imaging, Powder Technol. 69 (1992) 255–277.
[15] A. Bakshi, C. Altantzis, L.R. Glicksman, A.F. Ghoniem, Gas-flow distribution in bubbling fluidized beds: CFD-based analysis and impact of operating conditions, Powder Technol. 316 (2017) 500–511.
[16] J.G. Yates, D.J. Cheesman, Y.A. Sergeev, Experimental observations of voidage digstribution round bubbles in a fluidized bed, Chem. Eng. Sci. 49 (1994) 1885–1893.
[17] J. Werther, J. Wein, Expansion behavior of gas fluidized beds in the turbulent regime, AIChe. Symp. Ser. 90 (301) (1994) 31–44.
[18] A.P. Collier, A.N. Hayhurst, J.L. Richardson, S.A. Scott, The heat transfer coefficient between a particle and a bed (packed or fluidised) of much larger particles, Chem. Eng. Sci. 59 (2004) 4613–4620.
[19] Z.Y. Zhou, A.B. Yu, P. Zulli, Particle scale study of heat transfer in packed and bubbling fluidized beds, AICHE J. 55 (2009) 868–884.
[20] S. Ergun, Fluid flow through packed columns, Chem. Eng. Prog. 48 (1952) 83–94.
[21] C.Y. Wen, Y.H. Yu, A generalized method for predicting the minimum fluidization velocity, AICHE J. 12 (1966) 610–612.
[22] A.P. Baskakov, V.M. Suprun, Determination of the convective component of the heat-transfer coefficient to a gas in a fluidized bed, Int. Chem. Eng. 12 (1972) 324–326.
[23] A.P. Baskakov, B.V. Berg, O.K. Vitt, N.F. Filippovsky, V.A. Kirakosyan, J. M. Goldobin, V.K. Maskaev, Heat transfer to objects immersed in fluidized beds, Powder Technol. 8 (1973) 273–282.
[24] N.M. Čatipović, Heat Transfer to Horizontal Tubes in Fluidized Beds: Experiments and Theory, Dr Thesis, Oregon State University, 1979.
[25] N. Wakao, S. Kaguei, T. Funazkri, Effect of fluid dispersion coefficients in packed beds, Chem. Eng. Sci. 34 (1979) 325–336.
[26] M.E. Aerov, O.M. Todes, Hydraulic and Thermal Fundamentals on the Operation of Apparatus with Static and Fluidized Particle Bed (in Russian), Chimia, Leningrad, 1968.
[27] N.I. Gelperin, V.G. Ainshtain, Heat transfer in fluidized beds, chapter 10, in: J. F. Davidson, D. Harrison (Eds.), Fluidization, Academic Press, London, 1971.
[28] S.S. Zabrodsky, N.V. Anonishin, A.L. Parnas, On fluidized bed-to-surface heat transfer, Can. J. Chem. Engn. 54 (1976) 52–58.
[29] M.M. Shah, General correlation for maximum heat transfer to surfaces submerged in gas-fluidized beds, Chem. Eng. Sci. 185 (2018) 127–140.
[30] S.C. Saxena, Heat transfer between immersed surfaces and gas-fluidized beds, in: Advances in Heat Transfer, Elsevier, 1989.
[31] K. Ofuchi, D. Kunii, Heat-transfer characteristics of packed beds with stagnant fluid, Int. J. Heat Mass Transf. 8 (1965) 749–757.
[32] P.K. Agarwal, R.D. la Nauze, Transfer processes local to te coal particle: a review of drying, devolatilization and mass transfer in fluidized bed combustion, Chem. Eng. Res. Des. 67 (1989) 457–480.
[33] F. Scala, Mass transfer to freely moving active particles in the dense phase of a gas fluidized bed of inert particles, Chem. Eng. Sci. 62 (2007) 4159–4176.
[34] W. Prins, Fluidized Bed Combustion of a Single Carbon Particle, Thesis, Twente University, 1987.
[35] A.P. Baskakov, N.F. Filipovskii, V.A. Munts, A.A. Ashikhmin, Temperature of particles heated in a fluidized bed of inert material, J. Eng. Phys. 52 (1987) 788–793.
[36] M.M. Shah, Two-Phase Heat Transfer, Chapter 9, John Wiley & Sons, 2021.
[37] P.K. Agarwal, Transport phenomena in multi-particle systems…IV heat transfer to a large freely moving particle in gas fluidized bed of smaller particles, Chem. Eng. Sci. 46 (1991) 1115–1127.
[38] J. Chao, J. Lu, H. Yang, M. Zhang, Q. Liu, Experimental study on the heat transfer coefficient between a freely moving sphere and a fluidized bed of small particles, Int. J. Heat Mass Transf. 80 (2015) 115–1125.
[39] L. von Berg, A. Soria-Verdugo, C. Hochenauer, R. Scharler, Evaluation of heat transfer models at various fluidization velocities for biomass pyrolysis conducted in a bubbling fluidized bed, Int. J. Heat Mass Transf. 160 (2020) 120175.
[40] S.S. Zabrodsky, Hydrodynamics and Heat Transfer in Fluidized Beds, MIT Press, Cambridge, Ma., 1966.
[41] H. Martin, Heat transfer between gas fluidized beds of solid particles and the surfaces of immersed heat exchanger elements part I and II, Chem. Eng. Process. 18 (1984) 157–169, and 199-223.
[42] O. Molerus, K.E. Wirth, Heat Transfer in Fluidized Beds, Chapman & Hall, London, 1997.
[43] F. di Natale, A. Lancia, R. Nigro, Surface-bed heat transfer in fluidised beds: effect of surface shape, Powder Technol. 174 (2007) 75–81.
[44] A. Stefanova, X.T. Bi, C.J. Lim, J.R. Grace, A probabilistic heat transfer model for turbulent fluidized beds, Powder Technol. 365 (2020) 163–171.
[45] A. Svensson, F. Johnsson, B. Leckner, Bottom bed regimes in a circulating fluidized bed boiler, Int. J. Multiphase Flow 22 (1996) 1187–1204.
[46] R. Sekret, W. Nowak, Analysis of the bottom part of a large technical scale circulating fluidized bed boiler, Arch. Thermodyn. 27 (2006) 31–52.
[47] R. Wunder, A. Mersmann, Wärmeübergang zwichen Gaswirbelschichten und senkrechten Austauchflächen, Synopse 672, Chem. Ing. Tech. 51 (1979) 241.
[48] S. Yagi, D. Kunii, Studies on effective thermal conductivities in packed beds, AICHE J. 3 (1957) 373–381.
[49] N. Decker, L.R. Glicksman, Heat transfer in large particle fluidized beds, Int. J. Heat Mass Transf. 26 (1983) 1307–1320.
[50] I.A. Gibson, C.J. Slim, Yaoyao Zheng, S.A. Scott, J.F. Davidson, A.N. Hayhurst, Chem. Engn. Res. Des. 135 (2018) 103–111.